Hyperfine Interactions

Interaction between the
electromagnetic moments of a nucleus
and electromagnetic fields acting on the nucleus

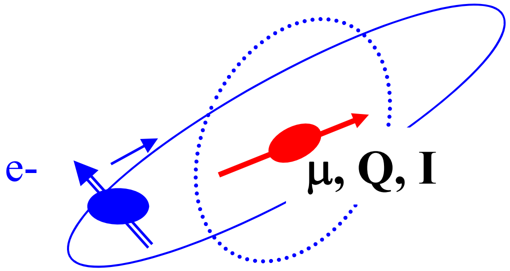

I = nuclear spin
μ = magn. dipole moment
Q = electric quadrupole moment

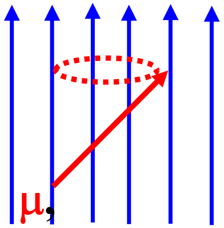

Magnetic field

magnetic HFI

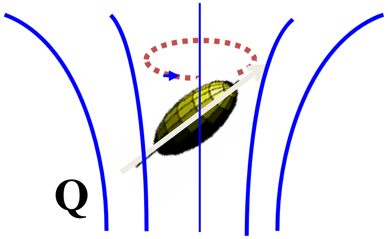

Electric field

electric HFI

Hyperfine Interactions

Electric and magnetic fields at nuclear sites may be produced by:

(i) **the electrons of the atom under consideration**
➔ **Hyperfine structure of optical transitions**

(ii) **External sources** (magnetic fields)
➔ nuclear structure studies

(iii) **The electrons of nearby atoms**
➔ **Information on chemical and solid state properties**

Hyperfine structure of electronic states of atoms

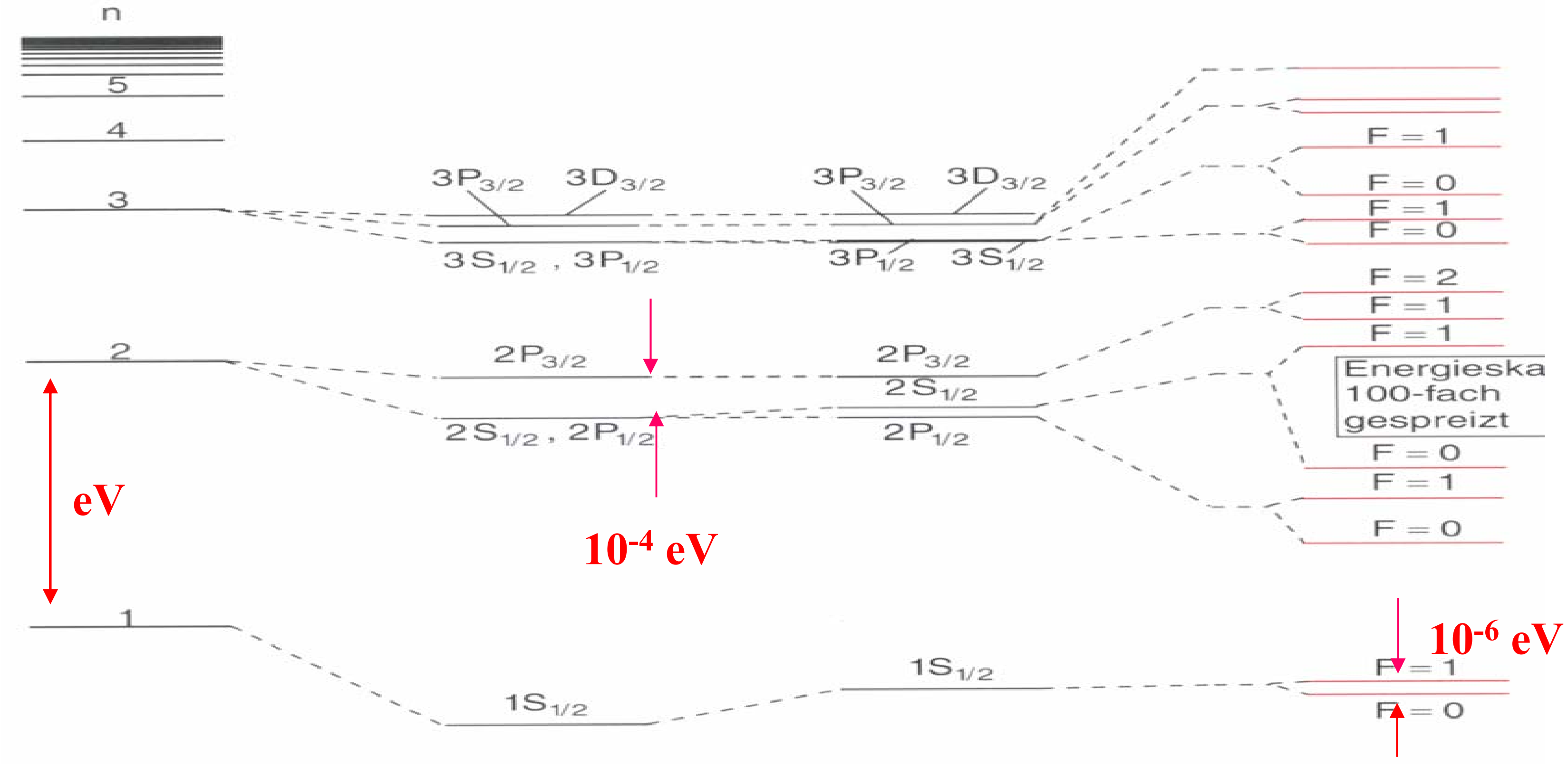

Bohr
Energy levels

Fine structure
Spin-orbit coupling

Hyperfine structure
nuclear effect

Order of magnitude of energies

eV	10^{-4} eV	10^{-6} eV

Hyperfine splitting of the D_2-line of Na

Detection in the resonance radiation of a Na-atomic beam excited by a frequency-variable dye laser

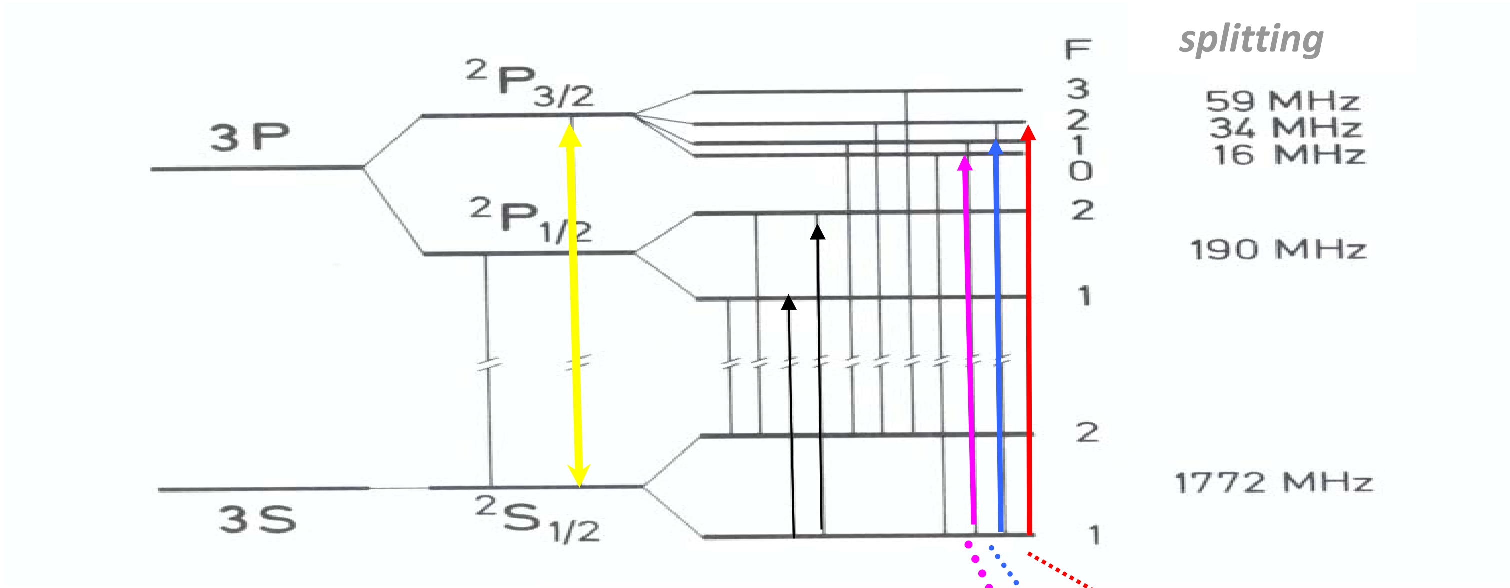

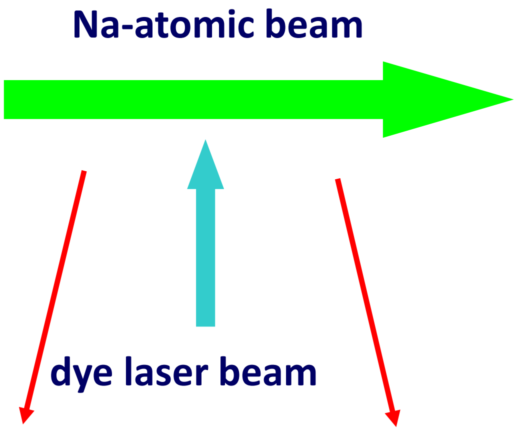

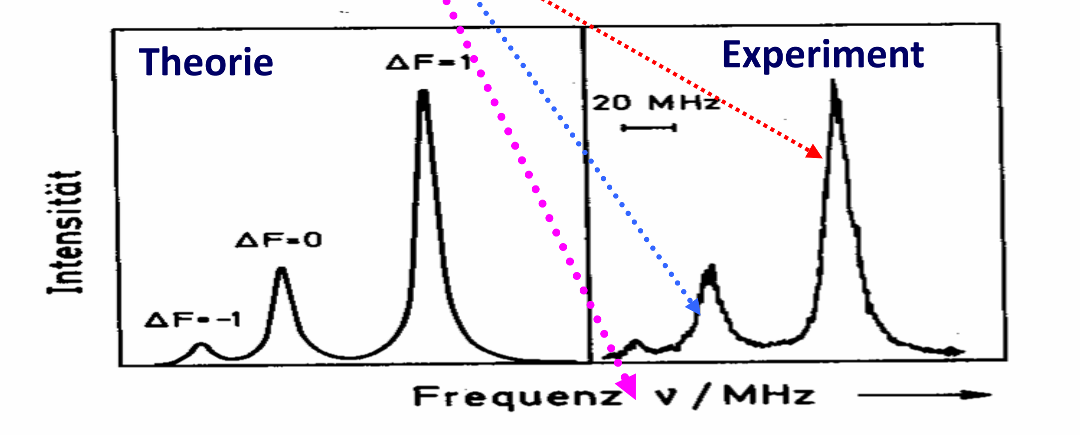

Hyperfine Interactions in Condensed Matter

Electric HF interactions

Static

non-cubic solids (metals,
semiconductors,isolators
Defects in cubic solids

Dynamic

Atomic motion in solids, liquids and
gases e.g. metal-hydrogen systems

Magnetic HF interactions

Static

Ferromagnets
Paramagnets at low temperatures
Knight Shift

Dynamic

Paramagnets at finite temperatures
Paramagnetische Lösungen
Spinfluctuations in ferromagnets

Electric Hyperfine Interaction

Interaction between the charge distribution of a nucleus $\rho_N(r)$ and the potential $\Phi(r)$ created by the charges surrounding the nucleus

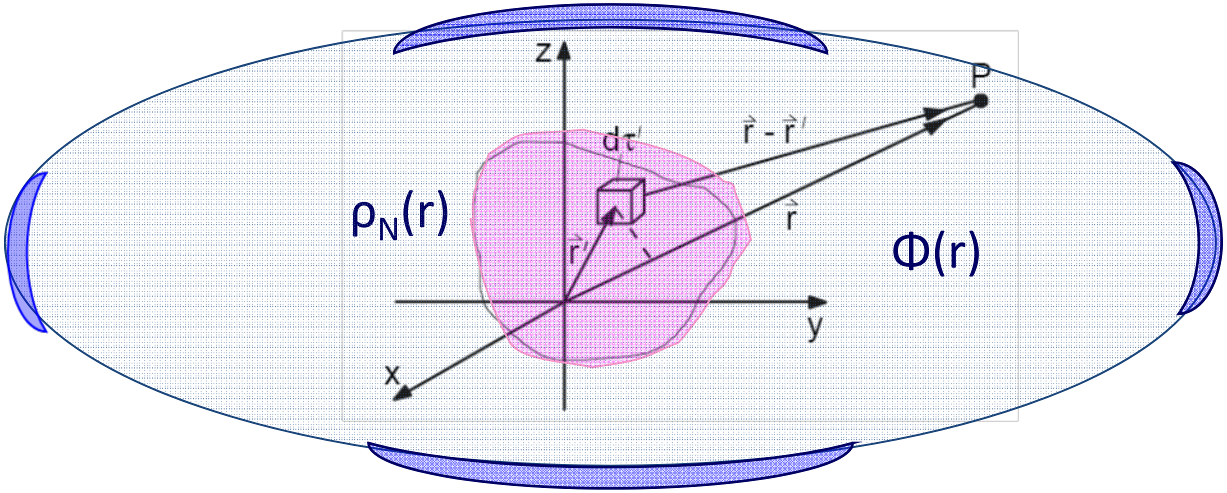

Interaction energy:

$$E_{el} = \int \rho_N(r)\, \Phi(r)\, d^3r$$

Nuclear charge distribution **potential**

Evaluation of the interaction integral

$$E_{el} = \int \rho_N(r)\, \Phi(r)\, d^3r$$

Expansion of the energy (into terms of decreasing magnitude):

$$E_{el} = \underset{\text{monopole term, point charge}}{E_{el}^{(0)}} + \underset{\text{dipole term = 0}}{E_{el}^{(1)}} + \underset{\text{quadrupole term}}{E_{el}^{(2)}} + \cdots$$

$$E_{el}^{(2)} = \frac{1}{2} \sum_{\alpha,\beta} \left(\frac{\delta^2 \Phi}{\delta x_\alpha\, \delta x_\beta} \right)_0 \int \rho_N(r)\, x_\alpha\, x_\beta\, d^3r$$

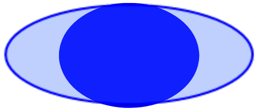

$$\Phi_{\alpha\beta} = \left(\frac{\partial^2 \Phi}{\partial x_\alpha\, \partial x_\beta} \right)$$

Tensor of the electric field gradient (EFG) →

$$\begin{pmatrix} \Phi_{\alpha\alpha} & \Phi_{\beta\alpha} & \Phi_{\gamma\alpha} \\ \Phi_{\alpha\beta} & \Phi_{\beta\beta} & \Phi_{\gamma\beta} \\ \Phi_{\alpha\gamma} & \Phi_{\beta\gamma} & \Phi_{\gamma\gamma} \end{pmatrix} \xrightarrow{\text{Principal axes transformation}} \begin{pmatrix} \Phi_{\alpha'\alpha'} & 0 & 0 \\ 0 & \Phi_{\beta'\beta'} & 0 \\ 0 & 0 & \Phi_{\gamma'\gamma'} \end{pmatrix}$$

The second order term of the energy

After principal axis-transformation (only diagonal terms):

$$E^{(2)}_{el} = \frac{1}{2}\sum_{\alpha}\left(\frac{\delta^2\Phi}{\delta x_\alpha^2}\right)_0 \int \rho_N(r)\, x_\alpha^2\, d^3r = \frac{1}{2}\sum_{\alpha}\Phi_{\alpha\alpha}\int \rho_N(r)\, x_\alpha^2\, d^3r$$

nuclear volume

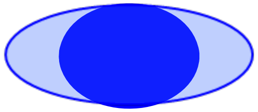

Decomposition of the nuclear volume into a spherical and a non-spherical part

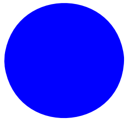

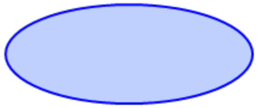

$$E^{(2)}_{el} = \underbrace{\frac{1}{6}\sum_{\alpha}\Phi_{\alpha\alpha}\int \rho_N(r)\, r^2\, d^3r}_{= E^{(2a)}_{el}} + \underbrace{\frac{1}{2}\sum_{\alpha}\Phi_{\alpha\alpha}\int \rho_N(r)[x_\alpha^2 - \frac{1}{3}r^2]\, d^3r}_{E^{(2b)}_{el} = \sum_{\alpha}\Phi_{\alpha\alpha}Q_{\alpha\alpha}}$$

Finite spherical nuclear volume | **Deviation from sphericity**

➔ Isotopie-(Isomerie-) shift | **➔ quadrupole splitting**

The electric quadrupole moment Q describes the deviation of the nuclear charge distribution from sphericity

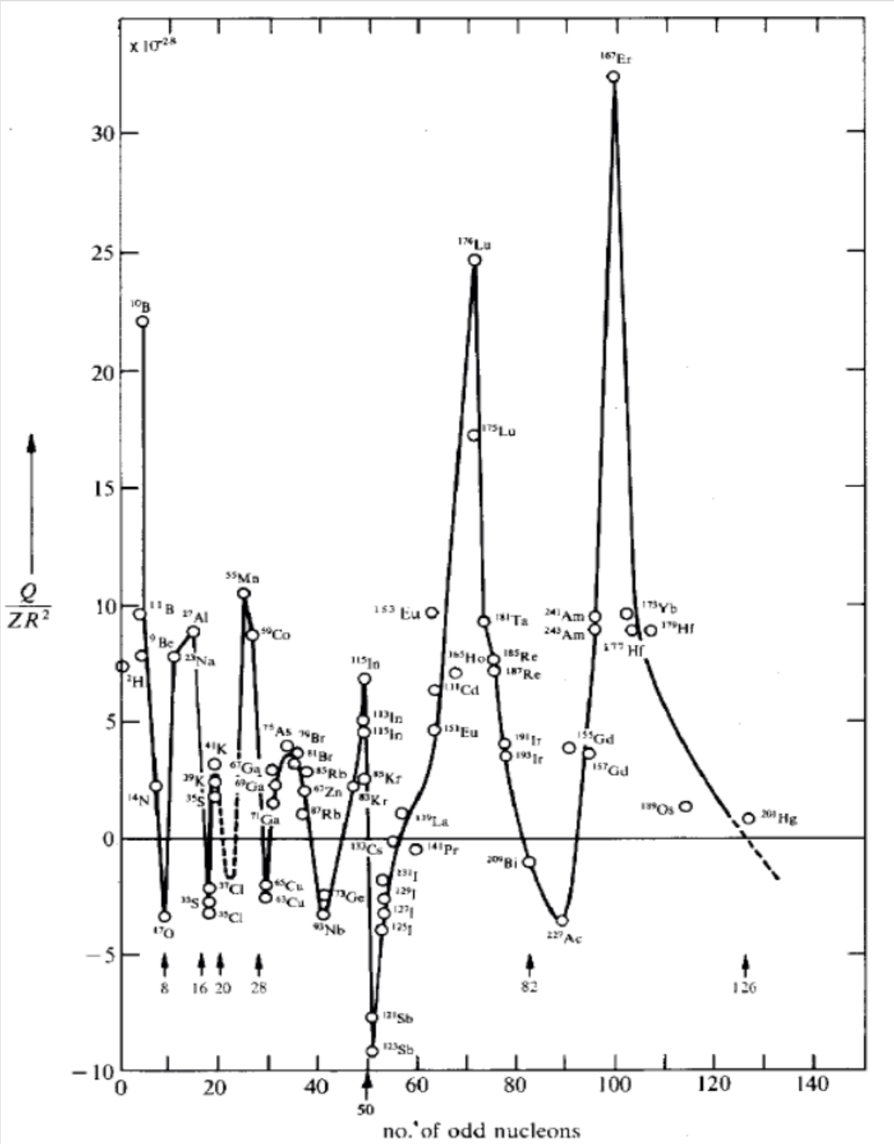

Classical definition:

$$\boxed{Q = Q_{zz} = \frac{1}{e}\int (3z^2 - r^2)\,\rho_N(\mathbf{r})\,d^3\mathbf{r}}$$

$$\boxed{\int \rho_N(\mathbf{r})\,d^3 r = Ze}$$

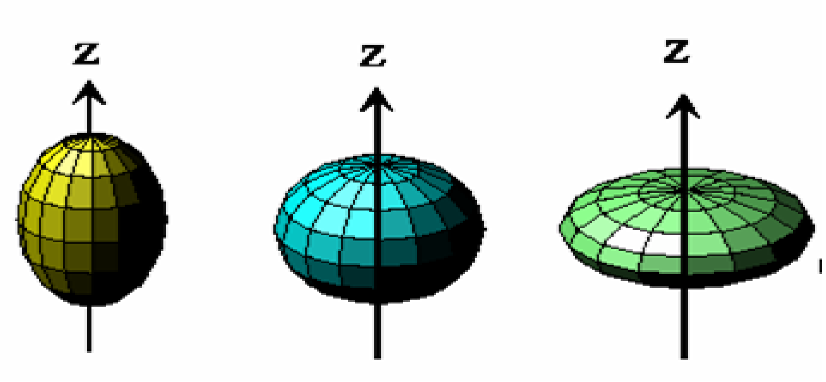

$Q > 0$ $Q = 0$ $Q < 0$

unit : barn (b) = 10^{-24} cm^2

The effect of the finite spherical charge distribution of the nucleus

$$E_{el}^{(2a)} = \frac{1}{6}(\Delta\Phi)_{r=0}\int \rho_N(r)\, r^2 d^3r$$

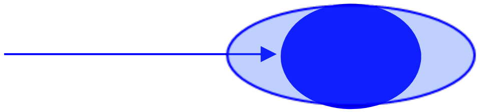

Possion equation $$(\Delta\Phi)_{r=0} = -\frac{\rho_{el}(0)}{\varepsilon_0} = \frac{Ze}{\varepsilon_0}\left|\Psi(0)\right|^2$$

Mean quadratic nuclear radius : $$\left\langle r_N^2 \right\rangle = \frac{1}{Ze}\int r^2 \rho_N(r)\, d^3r$$

Energy-shift caused by the finite nuclear size

$$\boxed{E_{el}^{(2\ \text{isomer})} = \frac{Ze^2}{6\varepsilon_0}\left|\Psi(0)\right|^2 \left\langle r_N^2 \right\rangle}$$

nuclear environment

nuclear radius parameter

Isotope- and Isomer shift

$$E_{el}^{(2a)} = \frac{Ze^2}{6\varepsilon_0} \left|\Psi(0)\right|^2 \left\langle r_N^2 \right\rangle$$

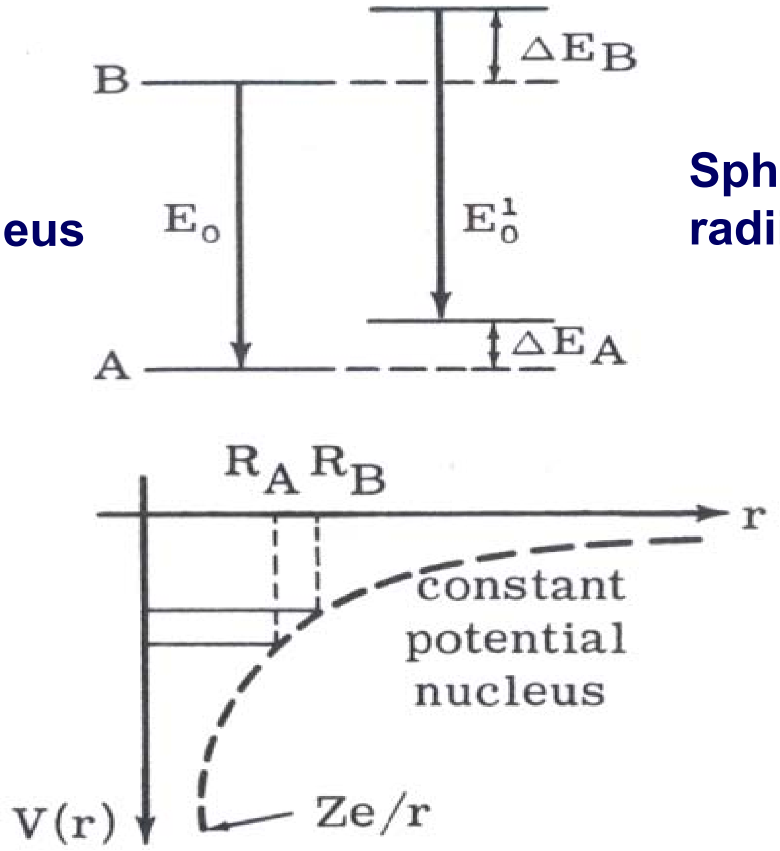

Point charge nucleus

Spherical nucleus with radii R_A, R_B in states A, B

The quadrupole interaction

$$E_Q^{(2)} = \frac{e}{6}\sum_{\alpha} V_{\alpha\alpha}\, Q_{\alpha\alpha}$$

The tensor of the electric field gradient (EFG) caused by charges outside the nucleus

$$\begin{pmatrix} V_{x'x'} & V_{x'y'} & V_{x'z'} \\ V_{y'x'} & V_{y'y'} & V_{y'z'} \\ V_{z'x'} & V_{z'y'} & V_{z'z'} \end{pmatrix}$$

Prinipal axes transformation

$$\begin{pmatrix} V_{xx} & & \\ & V_{yy} & \\ & & V_{zz} \end{pmatrix}$$

Choice of principal axes

$$|\mathbf{V_{xx}}| \leq |\mathbf{V_{yy}}| \leq |\mathbf{V_{zz}}|$$

Since $\sum_{\alpha} V_{\alpha\alpha} = 0$ the EFG is completely described by 2 parameters:

(i) Maximum component V_{zz}

(ii) Asymmetry parameter

$$\eta = \frac{V_{xx} - V_{yy}}{V_{zz}}, \ 0 \leq \eta \leq 1$$

The electric field gradient (EFG) produced by a point charge

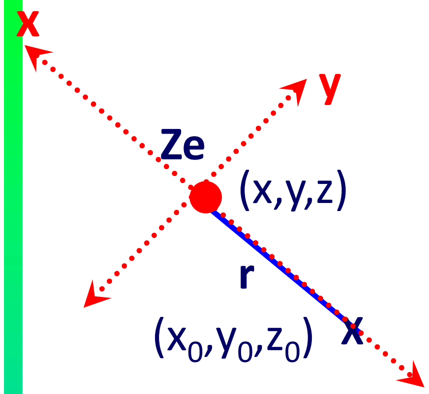

$$V(r)=\frac{Ze}{r}=\frac{Ze}{\sqrt{(x-x_0)^2+(y-y_0)^2+(z-z_0)^2}}$$

potential

$$V_x=\frac{\partial V}{\partial x}=Ze\frac{(x-x_0)}{((x-x_0)^2+(y-y_0)^2+(z-z_0)^2)^{3/2}}$$

x- component of the electric field

$$V_{xy}=\frac{\partial^2 V}{\partial x\,\partial y}=Ze\frac{3(x-x_0)(y-y_0)}{((x-x_0)^2+(y-y_0)^2+(z-z_0)^2)^{5/2}}$$

xy- component of the EFG tensor

$$V_{xx}=\frac{\partial^2 V}{\partial x^2}=Ze\frac{3(x-x_0)^2-r^2}{((x-x_0)^2+(y-y_0)^2+(z-z_0)^2)^{5/2}}$$

diagonal component of the EFG tensor

$$\begin{pmatrix} V_{xx} & V_{xy} & V_{xz} \\ V_{yx} & V_{yy} & V_{yz} \\ V_{zx} & V_{zy} & V_{zz} \end{pmatrix} \longrightarrow \frac{Ze}{r^5}\begin{pmatrix} 2r^2 & 0 & 0 \\ 0 & -r^2 & 0 \\ 0 & 0 & -r^2 \end{pmatrix}$$

$$V_{zz} = 2\,Ze/r^3$$

$$\eta=\frac{V_{xx}-V_{yy}}{V_{zz}}=0$$

The quadrupole splitting of nuclear states

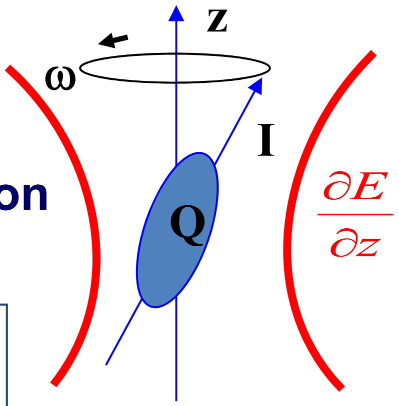

Classical description $E_Q^{(2)} = \frac{e}{6}\sum_{\alpha} V_{\alpha\alpha}\, Q_{\alpha\alpha}$ **Larmor precession**

Transition to quantum mechanics:
Spherical Tensor-Operators , Wigner-Eckart theorem

Hamiltonian of the QI $H_Q = \frac{eQV_{zz}}{4I(2I-1)}\{3I_z^2 - I(I+1) + \eta(I_x^2 - I_y^2)\}$

Eigenvalues for axial symmetrie of the EFG (η = 0)

$$E_Q^{(m)} = \frac{eQV_{zz}}{4I(2I-1)}\{3m^2 - I(I+1)\}$$

Axial asymmetry (η ≠ 0):
In most cases numerical diagonalisation of the QI Matrix $\langle I,m|H_Q|I,m'\rangle$ required

Quadrupole frequencies - definitions:

$$\omega_Q = \frac{eQV_{zz}}{4I(2I-1)\hbar} \quad \text{(Mrad/s)}$$

$$\nu_Q = \frac{eQ\,V_{zz}}{h} \quad \text{(MHz)}$$

Electric quadrupole interaction

Larmor precession

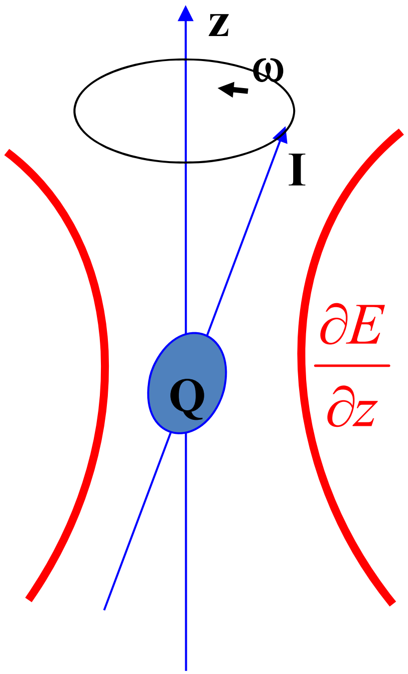

Quadrupole splitting

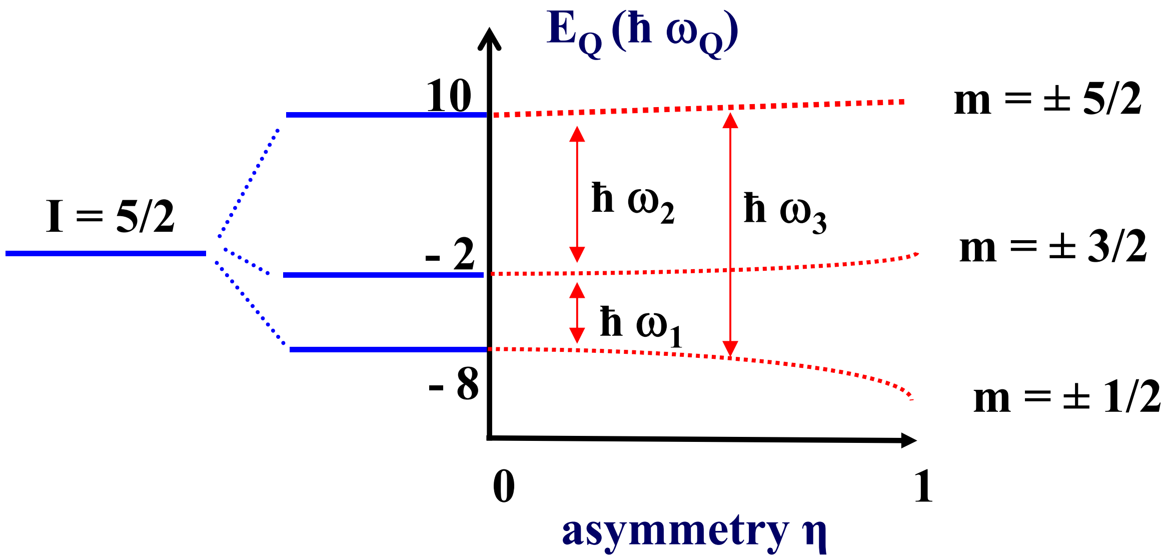

Order of magnitude of electric field gradients

$$E_Q = \hbar\omega_Q = \frac{eQV_{zz}}{4I(2I-1)} \longrightarrow V_{zz} = \frac{4I(2I-1)}{eQ} E_Q$$

Sensivity of HFI techniques: $E_Q \geq 10^{-8}$ eV

Assumption : Q = 1 b, I = 5/2

$$V_{zz} = \frac{10}{e \cdot 10^{-24}\ cm^2} 10^{-8}\, eV$$

$$V_{zz} \geq 10^{17}\ V/cm^2$$

Sources of electric field gradients of sufficient strength

- EFG produced by external charges is too weak
- **Charge distribution in solids** V_{zz}^{solid}
- Deformation of closed elctronic shells (1- γ_∞) V_{zz}^{solid}
  Sternheimer-Korrektur γ_∞ = 10 …. 70
- **Unclosed electronic shells with angular momentum J** $V_{zz} = -e\left\langle r^{-3}\right\rangle \cdot \left\langle J\|\alpha\|J\right\rangle \cdot J(2J-1)$
- Example: Rare earth ions (4f-elements); Dy^{3+}: 4f ^{9}, J = 15/2, **V_{zz} = $6 \cdot 10^{18}$ V/cm^2**

Phase Identification and Structure Information by Measurement of Electric Quadrupole Interaction - Example: ZrO_2

ZrO_2-structures

monoclinic

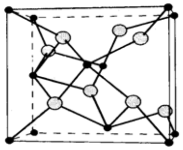

$\nu_q \neq 0$
$\eta \neq 0$

tetragonal

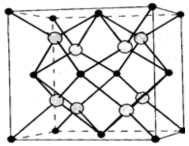

$\nu_q \neq 0$
$\eta = 0$

cubic

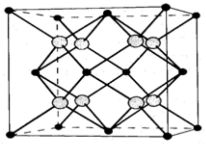

$\nu_q = 0$

Frequency and asymmetry

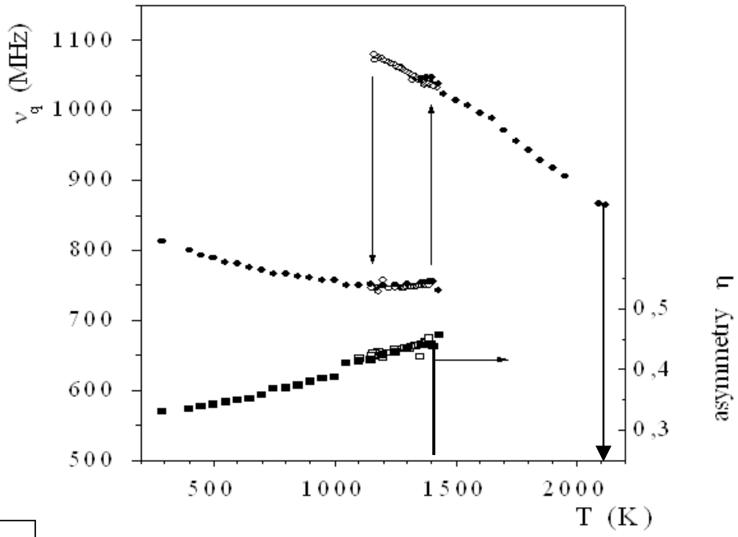

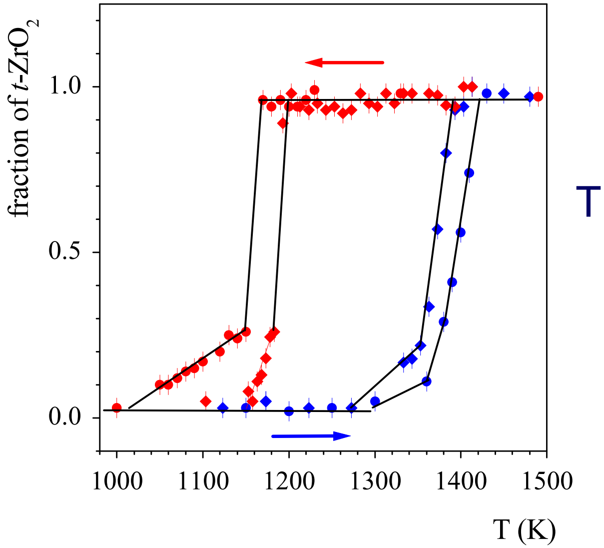

The *m* → *t* phase transition of ZrO_2

Magnetic Hyperfine interaction:

The interaction between nuclear magnetic dipole moments μ and magnetic fields B acting on the nucleus

$$\hbar\omega_m \sim \mu \cdot B$$

External field Bext

$B_{ext} \lesssim 20$ T

nuclear physics

determination of magnetic moments

Hyperfine Field B_{hf}

$B_{hf} \lesssim 10^3$ T

condensed matter physics

- unpaired spin density (magnetically ordered systems)
- Orbital and dipolar fields (ferro- and paramagnetic systems)

The Magnetic Splitting of Nuclear States

Hamilton Operator: $H_M = -\vec{\mu}\cdot\vec{B}_{hf}$

Energy Eigenvalues: $E_m = \langle I,m|-\mu_z B_z|I,m\rangle = -\gamma B_z \langle I,m|I_z|I,m\rangle = -g\mu_N B_z m$

Zeeman Splitting

equidistant $-I \leq m \leq I$

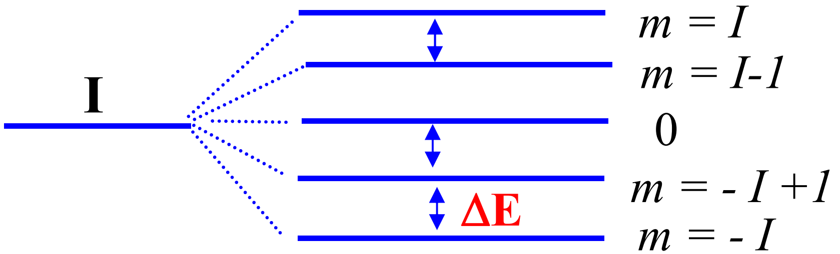

$\Delta E = g\,\mu_N Bz$
$= \hbar\,\omega_L$

Larmor-Precession

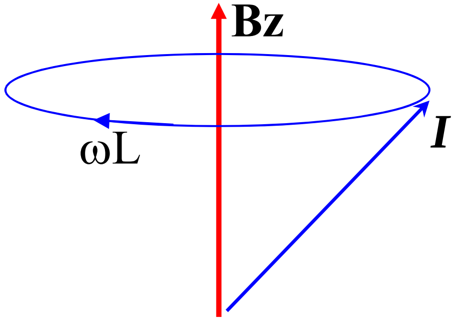

Larmor frequency

$\omega_L = \Delta E/\hbar = -g\,\mu_N Bz/\hbar$

Order of magnitude: B_{ext} = 100 kG, g = 1, μ_N = 3.15 10^{-12} eV/ G

$$\Delta E_M = \hbar\omega_L = g\,\mu_N\,B_{ext} = 3.15\cdot 10^{-7}\,\text{eV}$$

The nuclear parameter: the magnetic dipole moment μ

Moving charges = currents → magnetic moment

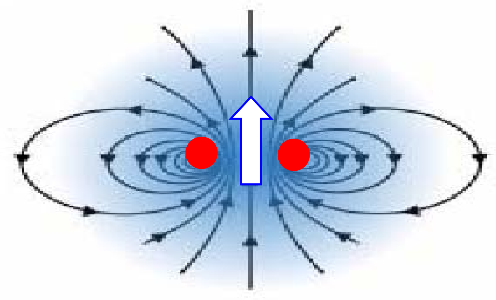

Classical example : Charge -e on an orbit with angular momentum I:

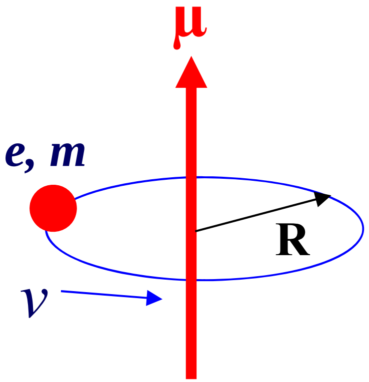

Definition of the magnetic moment:
μ = (1/c) circular current x area

Angular momentum: $\vec{I} = \vec{R} \, x \, \vec{p} = m_0 \, v \, R$

$$\vec{\mu} = -\frac{e}{2m_0c}\vec{I} = \gamma \, \vec{I}, \quad \gamma = \text{gyromagnetic ratio}, \quad I = \text{ang. momentum}$$

Magnetic Dipole Moments

Classical: $\vec{\mu} = -\frac{e}{2m_0c}\vec{I} = \gamma\,\vec{I},\quad \gamma = \text{gyromagnetic ratio},\quad I = \text{ang. momentum}$

Quantum mechanics for free-electron states ***|I, M=I>*** **:**

$$\mu = \langle I, M = I | \mu_z | I, M = I \rangle = \gamma\hbar I = g\,\mu_B I \qquad \mu_B = \frac{e\hbar}{2m_ec} = 5.788\,\text{x}10^{-15}\,\frac{\text{MeV}}{\text{Gauss}}$$

***g*-factor** **Bohr magneton**

Correspondingly for protons:

$$\mu_N = \frac{e\hbar}{2m_Nc} = 3.153\,\text{x}10^{-18}\,\frac{\text{MeV}}{\text{Gauss}}$$

$$\vec{\mu}_p = \frac{e\hbar}{2m_pc}\frac{\vec{I}}{\hbar} = g\,\mu_N\,\vec{I}$$

μ_N = nuclear magneton

Magnetic Dipole Moments

Free particles: $\vec{\mu}_{e,p} = g\,\mu_{B,N}\,\vec{I}$

g-factor	Elektron	Proton	Neutron
Orbital *l*: g_l	-1	1	0
Spin *s*: g_s	-2.0023	5,5856	-3,8263
g_s -Dirac theory	-2(1+α/2π+ ...)	1	0

anomalous

α = fine structure constant

For magnetic moments in nuclei, the spin-orbit coupling $\bar{l} + \vec{s}$ leads to the g factor

$$g = g_l \pm \frac{g_S - g_L}{2l+1} \quad for\ l \pm \frac{1}{2}$$

Experimental results and Schmidt lines

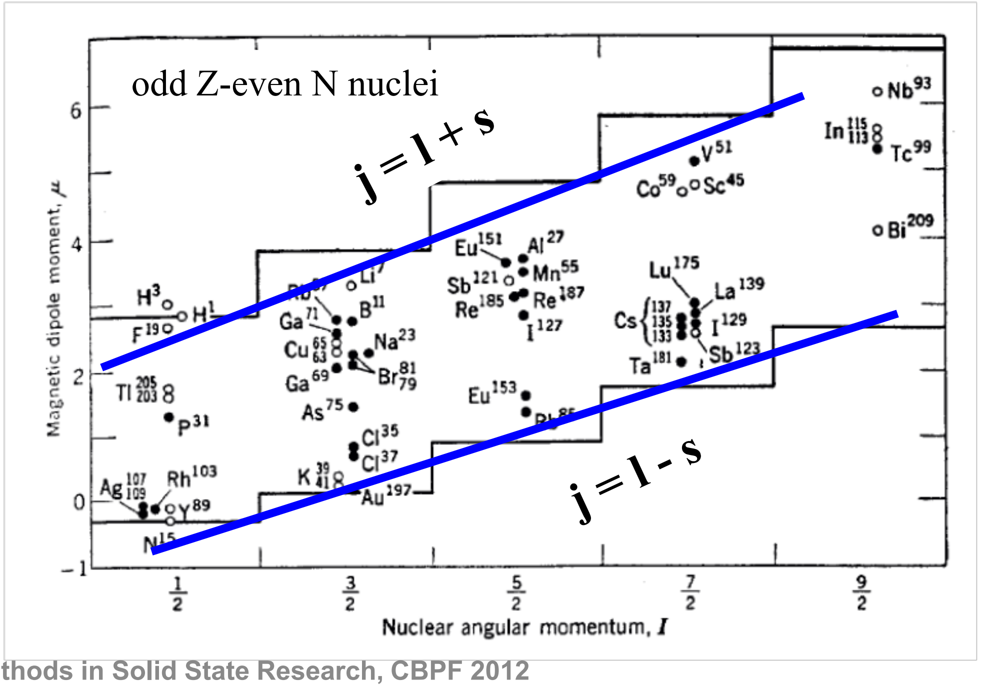

The magnetic hyperfine fielde B_{hf}

$$B_{hf} = B_{ext} + B_{orb} + B_{contact} + B_{dip} + B_{Lorentz} + B_{DM} + \ldots$$

Demagnetisation

External Field
$\leq$ 10 – 20 Tesla (100-200 KGauss)

Lorentz field

Dipolar field

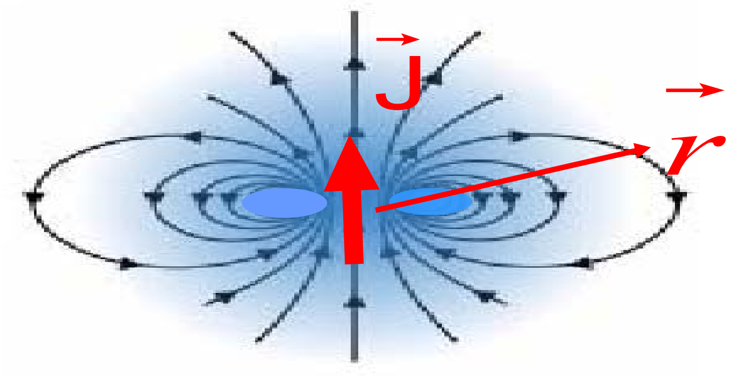

$$B_{dip} = -2\mu_B \frac{3\vec{r}\cdot(\vec{J}\cdot\vec{r}) - \vec{J}\cdot\vec{r}}{r^5}$$

$$r = 3\ \text{Å},\ J = 10 \longrightarrow B_{dip}^{max} \approx 1\ \text{Tesla}$$

The magnetic hyperfine field B_{hf}

$$B_{hf} = B_{ext} + B_{orb} + B_{contact} + B_{dip} + B_{Lorentz} + B_{DM} + \dots$$

Orbital field

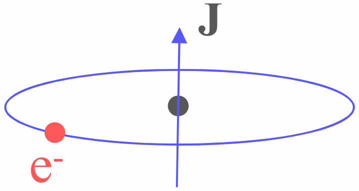

Angular momentum : $\vec{J} = \vec{L} + \vec{S}$

4*f*-elements (Gd, Tb, Dy…) : $J \leq 10$

$$B_{orb} = -2\mu_B \langle r^{-3} \rangle \langle J \| N \| J \rangle \langle J \rangle$$

Spin-orbit coupling $\langle J \| N \| J \rangle$

$B_{orb} \leq 10^3$ Tesla

The Fermi contact field

Field produced by s-electrons at the nuclear site: $B_C = 8\pi/3\ \mu_0 \mu_B |\Psi\uparrow(0)|^2$

In ferromagnets: $$B_{contact} = \frac{8\pi}{3} \mu_0\, \mu_B \underbrace{\sum_n [|\psi_{ns\uparrow}(0)|^2 - |\psi_{ns\downarrow}(0)|^2]}_{\text{spin-polarisation}}$$

B_C (Au in Fe)

= 10 ^{2} Tesla

spin-polarisation

Magnetic hyperfine fields in solids

Example: The magnetic 3*d*- and rare earth (4*f*-) metals

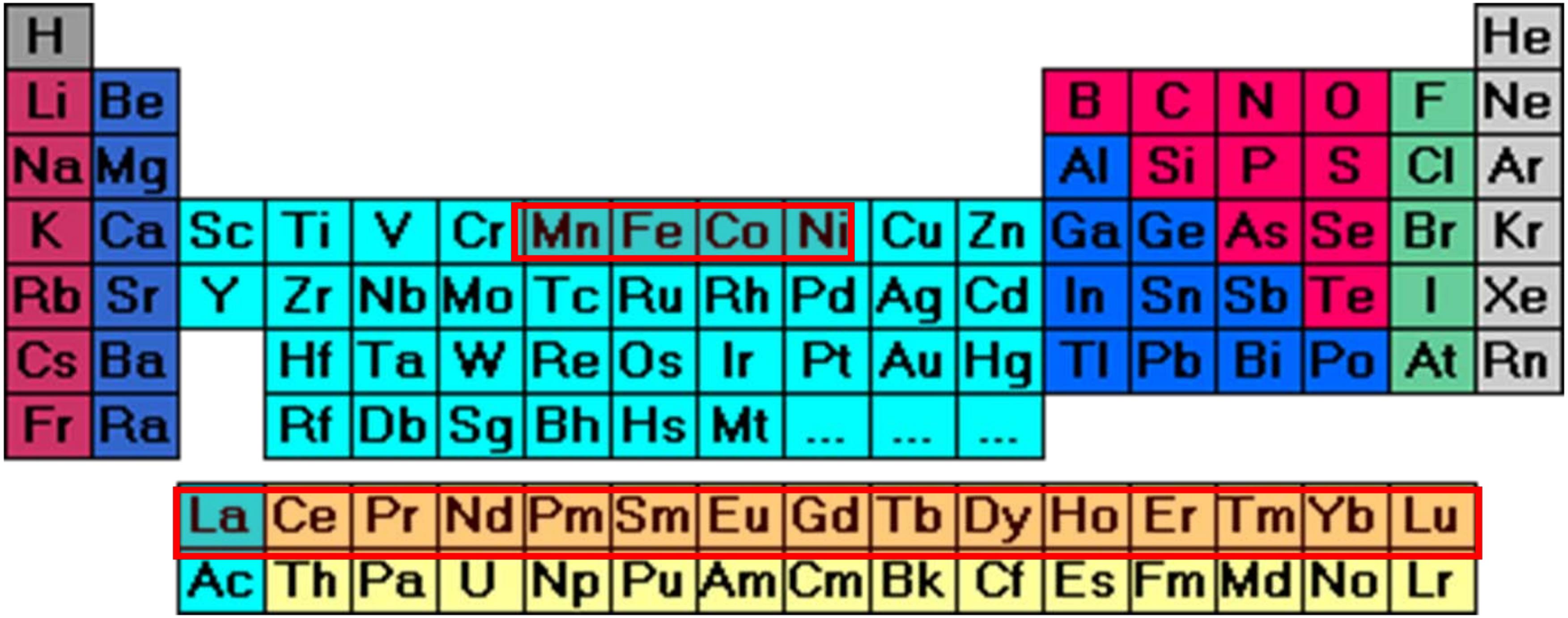

H																	He
Li	Be											B	C	N	O	F	Ne
Na	Mg											Al	Si	P	S	Cl	Ar
K	Ca	Sc	Ti	V	Cr	Mn	Fe	Co	Ni	Cu	Zn	Ga	Ge	As	Se	Br	Kr
Rb	Sr	Y	Zr	Nb	Mo	Tc	Ru	Rh	Pd	Ag	Cd	In	Sn	Sb	Te	I	Xe
Cs	Ba		Hf	Ta	W	Re	Os	Ir	Pt	Au	Hg	Tl	Pb	Bi	Po	At	Rn
Fr	Ra		Rf	Db	Sg	Bh	Hs	Mt	...	...	...						
		La	Ce	Pr	Nd	Pm	Sm	Eu	Gd	Tb	Dy	Ho	Er	Tm	Yb	Lu	
		Ac	Th	Pa	U	Np	Pu	Am	Cm	Bk	Cf	Es	Fm	Md	No	Lr	

3*d* ferromagnets Fe, Co, Ni : Stoner model

4*f* ferromagnets: RKKY theory of indirect coupling

Fe, Co, Ni - Stoner model of itinerant d-electron magnetism

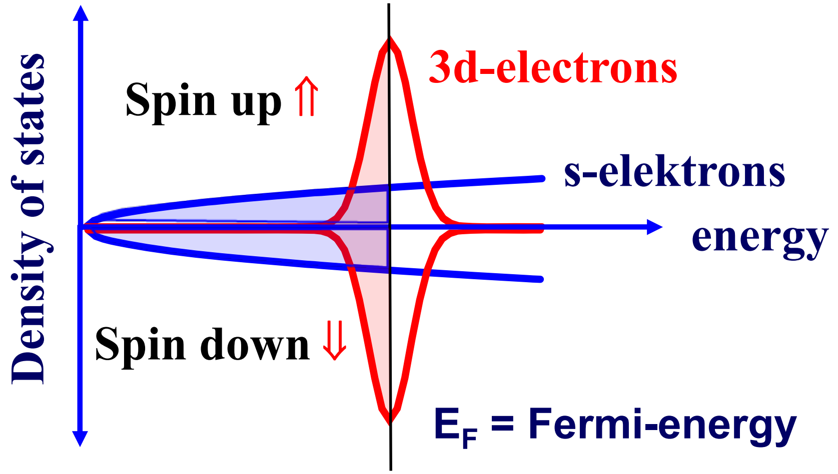

Bandstructure
of transition metals
(schematic)

$$n_{d\Uparrow} - n_{d\Downarrow} = 0\,;\, n_{s\Uparrow} - n_{s\Downarrow} = 0$$

Exchange interaction $H_{ex} = -J_{ex}\, S_{\Uparrow} \cdot S_{\Downarrow}$

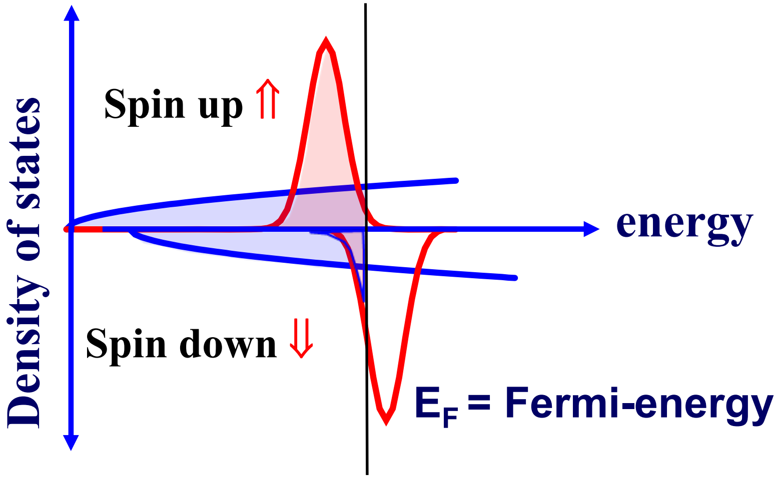

$$n_{S\Uparrow} - n_{S\Downarrow} = |\Psi_{S\Uparrow}(0)|^2 - |\Psi_{S\Downarrow}(0)|^2 > 0$$

→ Fermi contact field

$n_{d\Uparrow} - n_{d\Downarrow} > 0$ → d-moment

$$\mu_d = (n_{d\Uparrow} - n_{d\Downarrow})\,\mu_B$$

M. Forker, Nuclear Methods in Solid State Research, CBPF 2012

Hyperfine fields of different probe atoms in ferromagnetic Fe

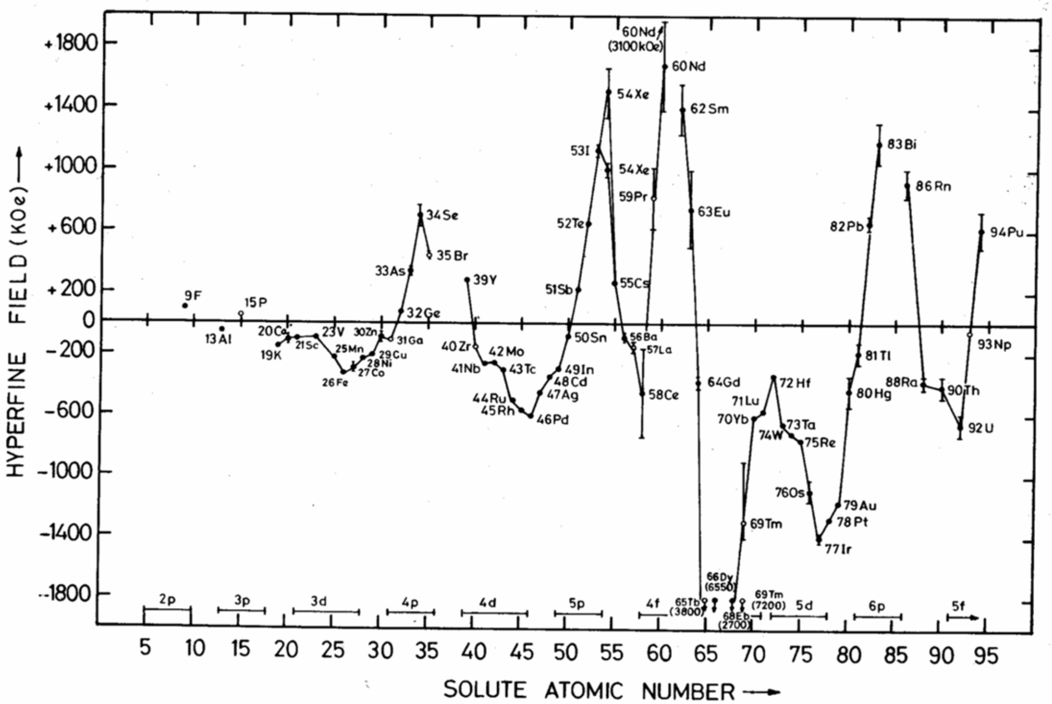

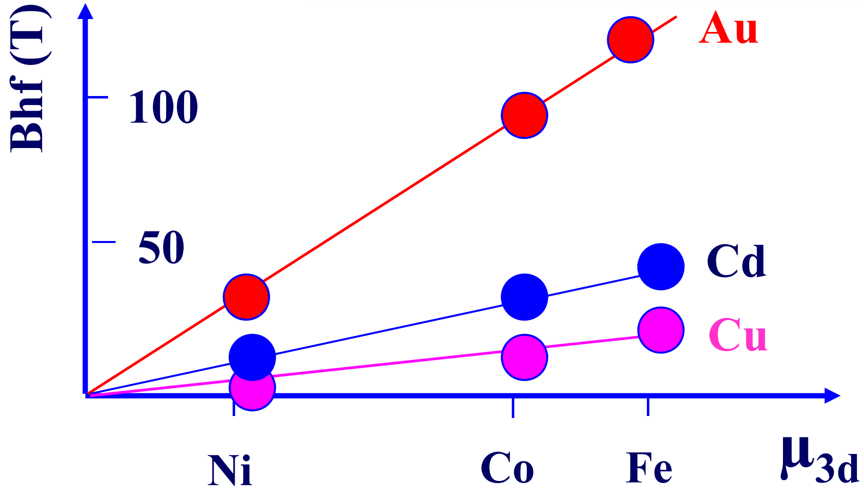

Hyperfine fields of the diamagnetic probes Au, Cd, Cu in the 3d ferromagnets Fe, Co, Ni

Illustration of the state of hyperfine field theory

Hyperfine fields at 4*d* and 5*sp* impurities in bcc iron

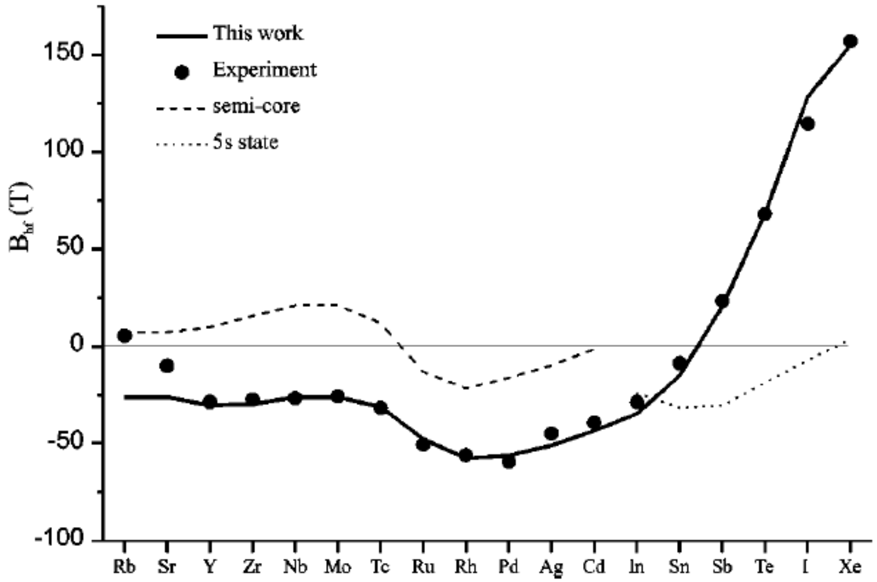

FIG. 3. Calculated hyperfine fields compared to experimental data. The semicore contributions (4*s* for Rb-Cd) and the contribution from the split-off 5*s* state (for In-Xe) are shown separately.

Cottenier and H. Haas, Phys. Rev. B 62 (2000) 46

The magnetic rare earth elements

The electronic configuration of the free atom : (Xe) $4f^{\mathrm{n}}$ $5d^2$ $6s^1$

Charge state in solids: mostly R^{3+} - (Xe) $4f^{\mathrm{n}}$
except Ce, Eu, Yb

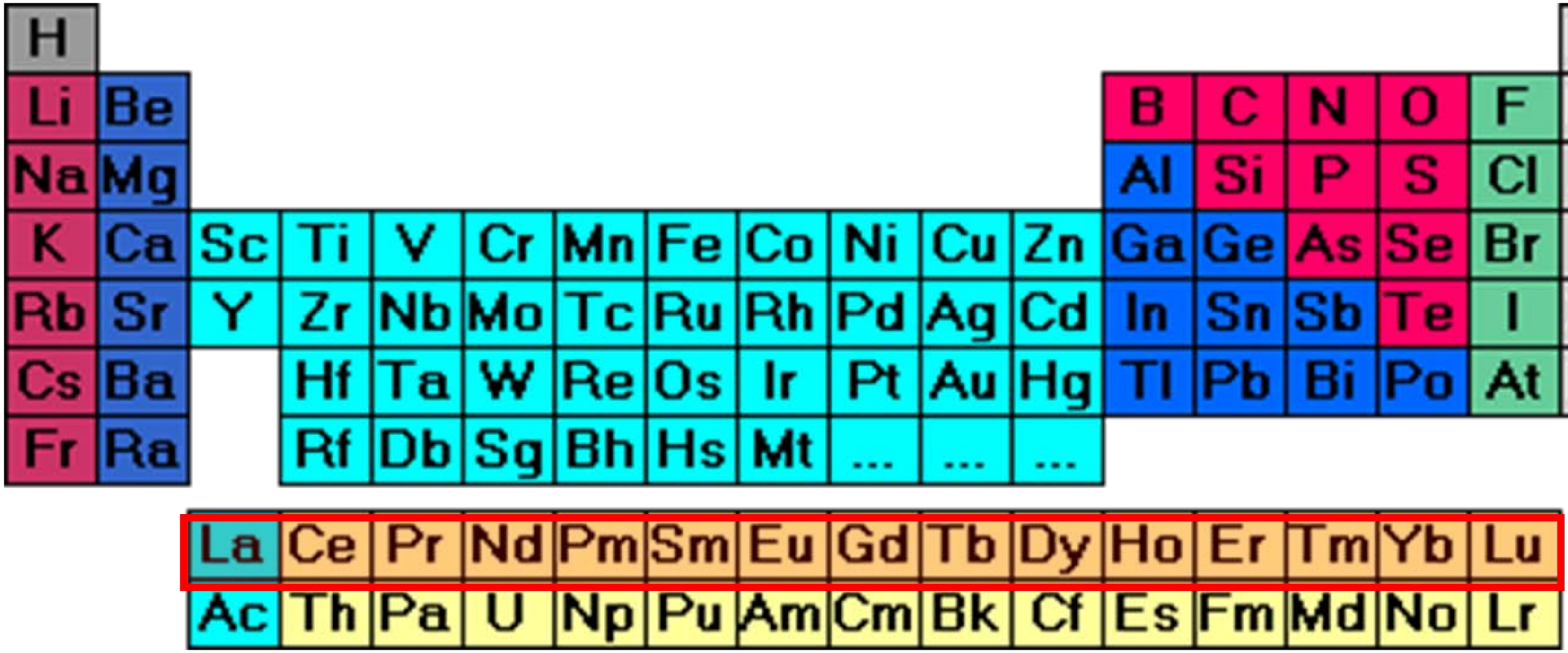

n: 0 1 2 3 4 5 6 7 8 9 10 11 12 13 14

M. Forker, Nuclear Methods in Solid State Research, CBPF 2012

Crystal and magnetic structures of the rare earth metals

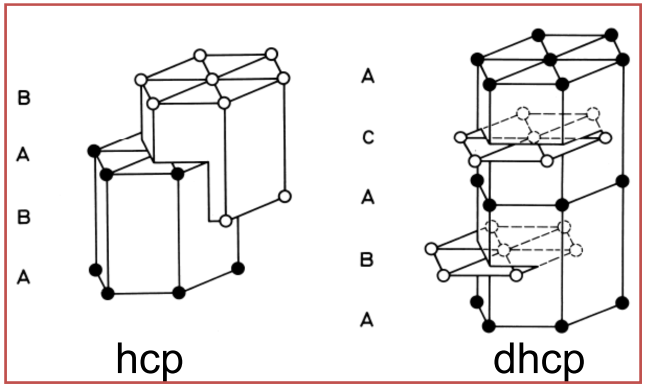

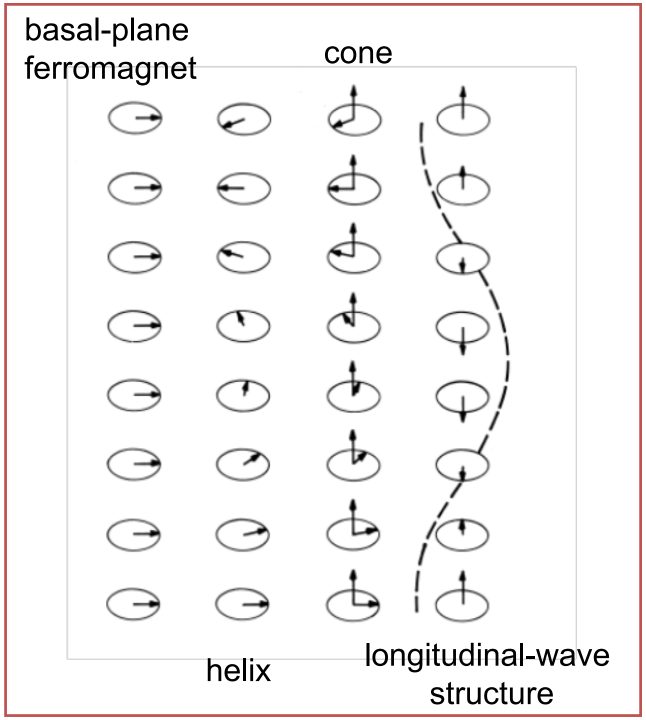

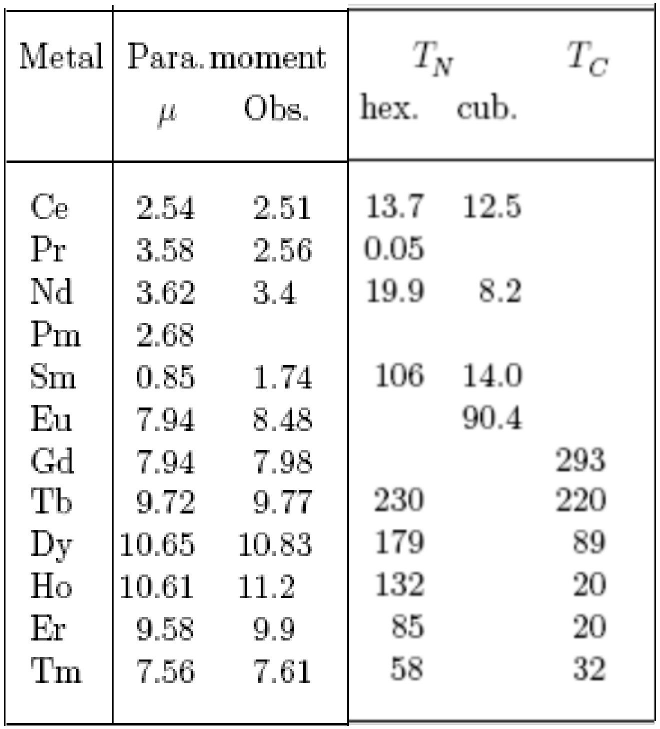

Metal	Para. moment μ	Obs.	T_N hex.	cub.	T_C
Ce	2.54	2.51	13.7	12.5	
Pr	3.58	2.56	0.05		
Nd	3.62	3.4	19.9	8.2	
Pm	2.68				
Sm	0.85	1.74	106	14.0	
Eu	7.94	8.48		90.4	
Gd	7.94	7.98			293
Tb	9.72	9.77	230		220
Dy	10.65	10.83	179		89
Ho	10.61	11.2	132		20
Er	9.58	9.9	85		20
Tm	7.56	7.61	58		32

The 4*f* wave function

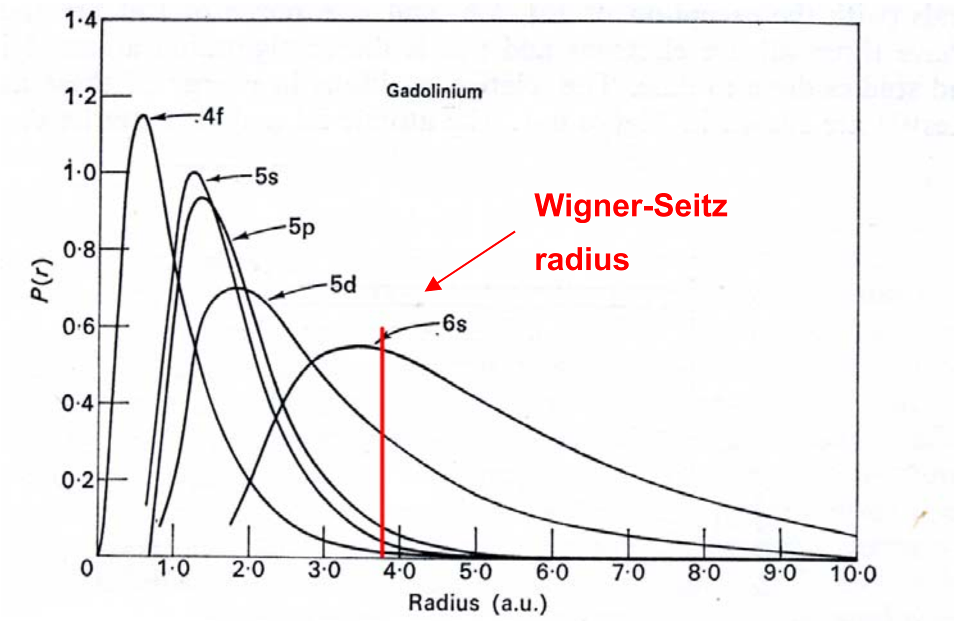

The 4*f* charge distribution

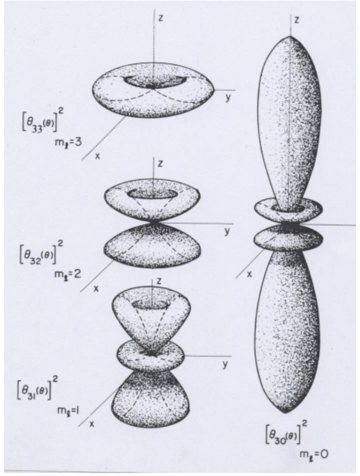

4*f* electrons:

- Inner electrons, highly localized within the Wigner Seitz cell
- strongly anisotropic charge distribution
- well protected by the outer shells

→

- pronounced chemical similarity
- orbital angular momentum unquenched
- strong crystal field interaction magnetically hard materials
- huge orbital fields at the *R* nuclei
- **very little 4*f*-4*f* overlapp**

Magnetic properties of R^{3+} ions

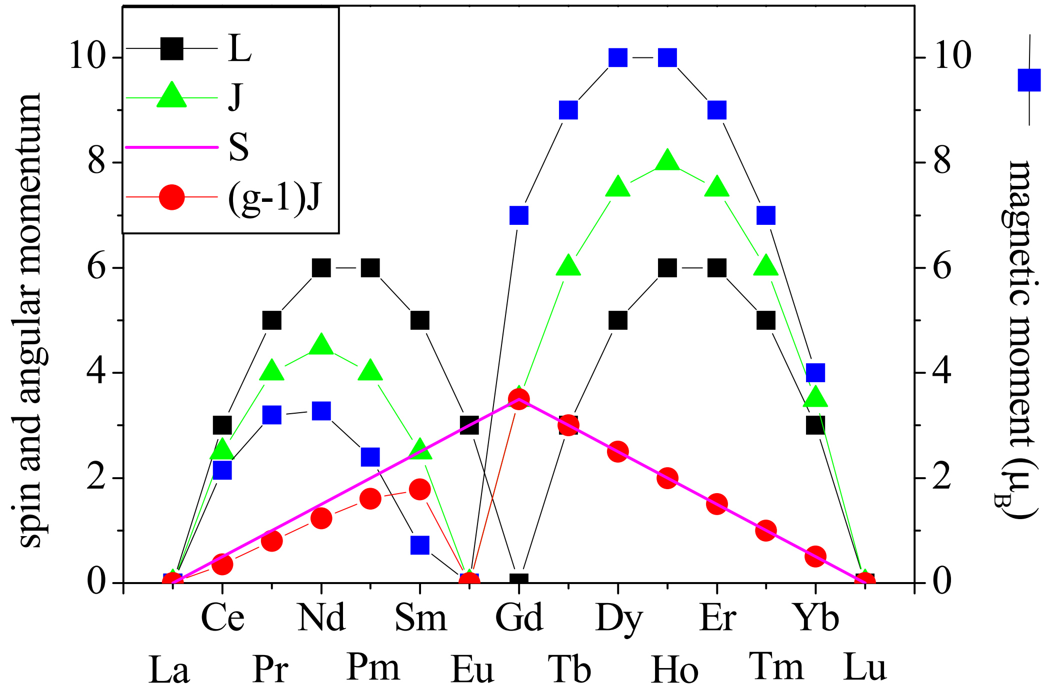

Russel-Saunders Coupling

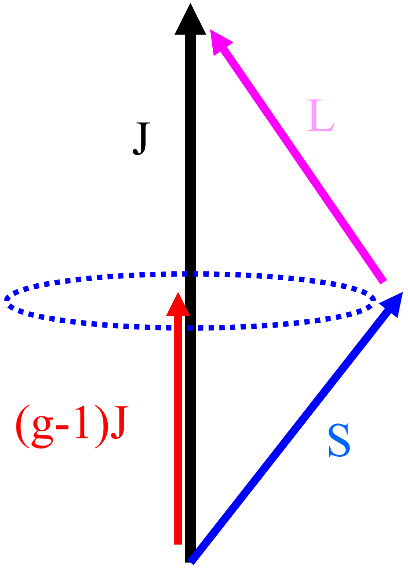

M. Forker, Nuclear Methods in Solid State Research, CBPF 2012

RKKY theory of indirect 4*f*-4*f* coupling

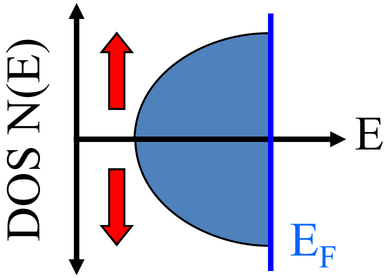

Exchange interaction between the 4*f* electrons and the *s*-conduction electrons

$$H_{sf} = -2\Gamma_{sf}\,\vec{s}\,\vec{S}$$

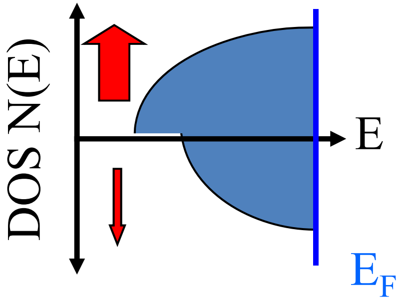

Spin polarisation of the s-conduction electrons $n\uparrow - n\downarrow > 0$

Kasuya, Yoshida

$$\rho(r) = n\uparrow - n\downarrow = -\frac{9\pi z^2 \Gamma_{sf}\left|\langle S_z\rangle\right|}{4E_F}\cdot\sum_i F(2k_F\cdot|(r-R_i)|)$$

$$B_{hf} \propto \Gamma_{sf}\left|\langle S_z\rangle\right|\sum_i F(2k_F R_i)$$

$$\left|\langle S_z\rangle\right| = (g-1)J$$

$$\boxed{B_{hf} \propto \Gamma_{sf}(g-1)J\sum_i F(2k_F R_i)}$$

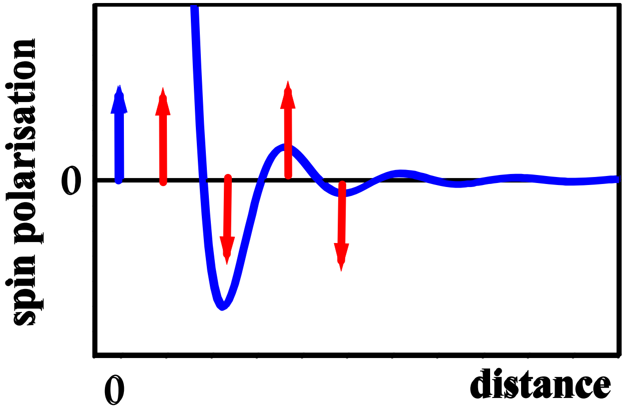

long-range, oscillating

Spin dependence of the ^{111}Cd hyperfine field in *R*Co$_2$ and *R*Al$_2$

$$B_{hf} \propto \Gamma(g-1)\sum_i F(2k_F R_i)$$